

LARGE EDDY SIMULATION OF ASH PARTICLE DEPOSITION AROUND TUBES OF A BOILER SUPERHEATER

Lourival Jorge Mendes Neto

Federal University of Santa Catarina, Department of Mechanical Engineering, Campus Trindade, Florianópolis, SC, Brazil 88040-900
mendes.lourival@gmail.com

João Luis Toste de Azevedo

Instituto Superior Técnico, Department of Mechanical Engineering, Av. Rovisco Pais, 1049-001 Lisboa, Portugal.
toste@ist.utl.pt

Edson Bazzo

Federal University of Santa Catarina, Department of Mechanical Engineering, Campus Trindade, Florianópolis, SC, Brazil 88040-900
ebazzo@emc.ufsc.br

Abstract. *Low rank coal is currently used in Brazilian thermal power plants. A number of problems are associated to the ash particle deposition on heat exchange surfaces causing unplanned shutdowns and reducing power output and plant efficiency. Several mechanisms involved in particulate and alkaline vapour deposition have been recently investigated by Knudsen (2001), such as inertial impact and vapour diffusion. The present work concentrates on inertial impact and investigates the deposition of particles around a circular tube based on Large Eddy Simulation. The turbulent flow is calculated based on two different grids and two subgrid models (Smagorinsky and dynamical model). Particle trajectories are traced in the Lagrangian framework based on one-way coupling and a discrete random walk model is used to simulate the subgrid-turbulence. Simulations are presented for one representative tube from the superheater of Jorge Lacerda thermo power plant to evaluate the hitting rate of particles with different diameters. The deposition rate of the particle around the cylinder is the input for particle deposition models.*

Key words: *Large eddy simulation, Particle deposition, Ash deposit, Coal, Boiler.*

1. Introduction

The use of low rank coal in boilers has many consequences. One of the primary problems associated with the use of coal is the deposition of fly ash on heat transfer surfaces. All coals have a significant content of ash, forming inorganic material, which can not be economically removed before combustion. This material forms deposits on the surface of the heat exchanger tubes and on the walls, causing unplanned shutdowns and reducing power output and efficiency of the boiler.

Nowadays, thermal power plants account for 21% of the Brazilian energy matrix and in future it is expected to have an increase to 60%. Coal as a fuel is expected to represent 10% of the installed capacity in the next years (ANEEL, 2006). The coal used as fuel for thermal power generation is mostly provided from the southern of Brazil and 42% of the annual production comes from Santa Catarina. The possible savings that could be made by better control of ash deposition in coal fired boilers in the US have been estimated at 400 million US\$/yr (*apud* Bouris et al, 2001).

In this context, the present paper has the objective of providing a detailed description of the gas-particle flow around one tube from a heat exchanger, based on conditions from the Jorge Lacerda thermo power plant. The approach used here is to analyse the flow and temperature distribution around a single tube based on large eddy simulation. All the calculations were performed using the commercial code FLUENT, (Fluent Inc. 2005).

The flow around bluff bodies is characterized by complex interactions between different phenomena such as boundary layers, separation and reattachment, shear layers, large two and/or three dimensional vertical structures, etc. Although models based on the Reynolds Average Navier Stokes equations (RANS) have been applied successfully in many practical computations, these tend to fail for flows involving large unsteady structures. The Large Eddy Simulation (LES) approach has a better potential to determine these complex structures and interactions between the flow field and the bluff body (Fröhlich *et al*, 1998).

Many studies involve comparison between LES and RANS (*apud* Fröhlich, *et al*, 1998 and Lübcke *et al*, 2001). The superiority of the LES predictions is attributed to the fact that LES is better suited to flows where the size of the eddy (integral length scale of the turbulence) is comparable to that of the obstacles in the flow. In fact the LES approach involves the direct solution of the large vortices and only the vertical structures with size below the filter size are modelled. This is a primary advantage, since the influence of the turbulence model is reduced; in contrast, it significantly increases the computational effort in comparison to RANS (Fröhlich *et al*, 1998 and Lübcke *et al*, 2001).

In LES, the large eddies that depends strongly on the flow configuration and its boundary conditions are resolved numerically whereas only the fine scale turbulence has to be modelled by a subgrid scale model. The Large Eddy Simulation method solves the Navier Stokes equations by a spatial average over a small volume. Due to the non-linearity of the Navier Stokes equations its average forms contains additional terms for which models are needed, these are termed subgrid or subfilter scale models, (Franke and Frank, 2002).

Mostly two subgrid models are commonly used, the Smagorinsky subgrid scale model (SM) and the dynamic Smagorinsky model (DSM) of Germano *et al*, (1991). Both models are based on the Boussinesq hypothesis; they depend on the turbulent viscosity and this viscosity is assumed as proportional to the strain rate tensor.

Understanding the large scale vortex dynamics it is possible to predict the particle dispersion in a bluff body flow. This is of a great significance, once the ash deposition depends on the interaction of the particle with the vortex structure behind the tube.

The particle trajectories were traced in a Lagrangian framework based on one way coupling, it means that they do not affect the gas flow. The particle tracking used here is the Discrete Random Walk (DRW), based on the Eddy Life Time model.

The present work is organized as follows: Following this introduction, the numerical methodology is briefly discussed and the test cases are presented. The impact of the grid on the LES calculation is analysed by comparing the results of two three-dimensional 3D different grids and a two-dimensional (2D) grid. The particle deposition is analysed considering the stochastic model of the DRW and without it. At the end, the paper discusses the impact of the analysis in the first tube of an in-line tube arrangement of the boiler resulting in a deposition rate that can be considered in a deposition model such as those presented by Mendes *et al*, (2006).

2. Modelling Approach

The Large Eddy Simulation (LES) is an intermediate methodology between the Direct Numerical Simulation (DNS) and the Reynolds Averaged Navier Stokes (RANS) equations. In the DNS approach, the Navier Stokes equations are solved by a numerical methodology resolving the smallest scale in turbulent flow, namely the Kolmogorov length and time scale (Breuer, 1998; Lübcke *et al*, 2001; Franke and Frank, 2002; Silveira, 2002). In the framework of RANS all aspects of turbulence are modelled, which enhances the numerical efficiency at the expense of a strong model dependency.

As opposed to the RANS approach, a major portion of the turbulence scales is numerically resolved within LES. Both methods solve averaged Navier Stokes equations, both on time and space. In the LES framework calculations are done along time and therefore the average over time is limited to the calculation time step, while the averaging in space is dictated by the grid resolution. Due to the non linearity of the Navier Stokes equations their average forms contain additional terms for which models are needed. They are termed turbulence models in RANS and subgrid or subfilter scale models in LES. The filtered incompressible equations used in LES approach are:

$$\frac{\partial \bar{u}_i}{\partial x_i} = 0, \quad (1)$$

$$\frac{\partial \bar{u}_i}{\partial t} + \frac{\partial \bar{u}_i \bar{u}_j}{\partial x_j} = -\frac{1}{\rho} \frac{\partial \bar{p}}{\partial x_i} - \frac{\partial \tau_{ij}}{\partial x_j} + \nu \frac{\partial^2 \bar{u}_i}{\partial x_j \partial x_j}, \quad (2)$$

where \bar{u}_i, \bar{p}, ρ denote the filtered velocity, pressure and density. The viscous stress is given by $\tau_{ij} = \overline{u_i u_j} - \bar{u}_i \bar{u}_j$.

The filtering procedure provides the governing equations for the resolvable scales of the flow field. They include an additional term for the non resolvable subgrid scale stress which describes the influence of the small scale structures in the larger eddies. To model these non resolvable subgrid scales two different models are applied namely the Smagorinsky model and the dynamic model proposed by Germano *et al* (1991). Both use an eddy viscosity concept, the main difference being the choice of the *ad-hoc* constant by the Smagorinsky model or a dynamic function in the Germano model.

The effective conductivity in the energy equation is the sum of the molecular conductivity of the fluid and the turbulent contribution related to the eddy viscosity by the turbulent Prandtl number, here assumed as 0.7.

2.1. Smagorinsky Eddy Viscosity Model

The Smagorinsky model employs the Boussinesq approximation, which means that the Reynolds stresses is considered proportional to an eddy viscosity and the velocity gradient. The Reynolds tensor can be written as a function of the filtered velocity field and turbulent kinetic energy by (Silveira, 2002):

$$\tau_{ij} = -v_t \left(\frac{\partial \bar{u}_i}{\partial x_j} + \frac{\partial \bar{u}_j}{\partial x_i} \right) + \frac{2}{3} k \delta_{ij}, \quad (3)$$

where v_t , k , δ_{ij} are the eddy viscosity, turbulent kinetic energy and the Kronecker delta. The turbulent kinetic energy subgrid can be incorporated with pressure resulting in a modified pressure term. The eddy viscosity can be modelled by:

$$v_t = (C_S \Delta)^2 |\bar{S}|, \quad (4)$$

where C_S is the Smagorinsky constant, here used as been 0.1, Δ is the filter width of the box filtering method, obtained from the volume of the computational cells and S the strain rate tensor, $|\bar{S}| = \sqrt{2\bar{S}_{ij}\bar{S}_{ij}}$.

This model tends to fail if applied to the flow near the walls and transition flows where the separation of the boundary layer occurs determining the generation of large vortices. Therefore the Germano dynamic model is also considered.

2.2. Dynamic Eddy Viscosity Model

Dynamic models are sensitive to the local state of the flow and thus predict more accurately transition and have the correct near wall behaviour as opposed to the constant coefficient Smagorinsky model. The dynamic model overcomes this limitation of the dependence of an *ad hoc* constant imposed by making use of two different filters, the grid filter and the test filter.

The filtering process consists of filtering the Navier Stokes equations by using a filter width similar to the grid size followed by the same filtering process but with a filter width two times larger than the first one, know as test filter. Based on this concept it is possible to note that the dynamic model makes use of the lower resolved scales, situated between the two filters, to model the energy transfer between the resolved and non resolved scales. This is obtained by minimizing the mean square error in the Germano identity, which equals the difference between the subgrid and subtest tensor to the Leonard tensor. This process of filtering is described elsewhere (Saugaut and Grohens, 1999; Silveira, 2002).

2.3. Particle Phase

The mass flux of the ash particles inside the boiler, calculated by Reinaldo (2004), is $\dot{G}_p = 0.07$ [kg/m²/s]. This flux compared with the gas flux, $\dot{G}_g = 1.5$ [kg/m²/s] leads to a mass loading of 4.8%. The ash content of the coal used in the boiler is about 41%, in dry basis, so one possible estimative is that the density of the ash particles can be around of 41% of the coal density in dry basis, resulting in 535 kg/m³. Besides if compared to the gas density ($\rho_p/\rho_g \cong 10^3$), the particle concentration in volume can be estimated as 10^{-5} . In these conditions inter-particle effects are negligible and it is close to the limit where the effect of particles in the gas flow can be neglected (10^{-6}).

Based on the high density ratio the Basset force and the added mass term are small and are therefore neglected. The ratio of the lift to drag force is given by the relation between the Saffman and drag force $F_{Saff}/F_{drag} \cong d_p^2 (du/dy)^{0.5} / \mu$, where d_p , du/dy , μ are the diameter of the particle, the derivate of the gas velocity and the molecular viscosity of the gas. For particles with small diameter and low inertia this force can be neglected in comparison to the drag force, (Crowe, 1979). Under these assumptions, the Lagrangian equations governing the particle motion become:

$$\frac{dx_p}{dt} = u_p, \quad (5)$$

$$\frac{du_p}{dt} = \frac{f}{St_p} (u - u_p), \quad (6)$$

where f is a correction factor for large Reynolds number of the drag coefficient, here considered from spherical particle. St_p is the particle Stokes number defined as

$$St_p = \frac{\tau_p}{\tau_f} = \frac{\rho_p d_p^2}{18\mu} / D/U_\infty, \quad (7)$$

where τ_p , τ_f , are the particle relaxation time [s] and the mean flow time scale [s].

As the flow is turbulent and only the large eddy are solved through LES approach. The fluctuating gas flow velocity considered using the stochastic method in the Discrete Random Walk model (DRW). In this model, the fluctuating velocity components are discrete piecewise constant functions in time. Their random value is selected from a Gaussian distribution and is kept constant over an interval time given by the characteristic lifetime of eddies. Further details can be found on Fluent, 2005. The DRW is necessary for particle sizes with particle relaxation time comparable or smaller than the subgrid time scales. The particle flow simulation is based on the computed trajectories of .representative particles. The number of particles represented by each trajectory is based on the mass flow rate and the particle size distribution.

3. Numerical Methodology

The computational domain is described in a fixed Cartesian coordinate system (x, y, z). The y-axis is along the streamwise mean flow direction, the z-axis is along the spanwise direction and the x-axis is perpendicular to both y- and z-axis. The origin of the coordinate system and the size of the computational domain are shown in Fig.1.

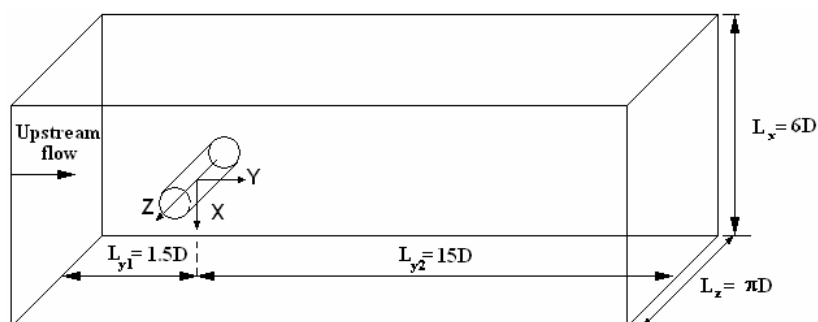


Figure 1. Physical configuration of the cylinder flow.

The diameter of the cylinder is 31.8 mm, the blockage ratio is 16%, close to the value used by the papers referred here. The spanwise direction is usually estimated from the experimental measurements or prior knowledge of the sizes of the streamwise vortex structures. Many authors have reported that the spanwise direction should be at least πD to represent the three dimensional structures (Frölich *et al*, 1998, Breuer, 1998, Lübcke *et al*, 2001, Liang and Papadakis, 2006).

In the present situation two meshes were used to analyse the grid dependence, A0 and A1. Further a 2D simulation (A2) was also carried out to analyse the 3D aspects of turbulence. For the finer grids, 32 layers are used in the spanwise direction with two different quantities of cells in the periphery of the cylinder, 128 and 256 cells for the coarse and finer mesh, respectively. A constant expansion of 1.1 is used for the cell spacing in the radial direction away from the cylinder wall with the smaller spacing in the radial direction being $\Delta r_{min}/D = 1.96 \times 10^{-2}$. The details about the cases considered are shown in Tab. 1. All calculations were performed under isothermal conditions except case B1S which is based in case A1S considering heat transfer.

Table 1. Overview of all simulations for the circular cylinder.

Run	N_{Total} Cells	Grid $N_x \times N_z$	Domain	Subgrid Model	L_r/D	y^+ (maximum)
A0D	206848	128x32	6Dx16.5Dx πD	Dynamic	1.45	4.00
A1D	370688	256x32	6Dx16.5Dx πD	Dynamic	1.05	4.25
A2D	60928	128x8	6Dx16.5Dx $\pi/4D$	Dynamic	–	6.00
A0S	206848	128x32	6Dx16.5Dx πD	Smagorinsky	0.75	4.50
A1S	370688	256x32	6Dx16.5Dx πD	Smagorinsky	1.35	4.35
A2S	60928	128x8	6Dx16.5Dx $\pi/4D$	Smagorinsky	–	5.85
B1S	370688	256x32	6Dx16.5Dx πD	Smagorinsky	1.00	4.85

The smaller spacing in the radial direction was determined considering the Taylor microscale, λ [m]. The Taylor scale is located between the flow integral scale and the Kolmogorov scale and can be estimated by (Arpaci, 1997):

$$\frac{\lambda}{D} = \frac{1}{\sqrt{Re_D}} \quad (8)$$

Re_D is the Reynolds number based on the diameter of the tube, D [m]. Considering the inlet velocity of 10 m/s with a gas temperature of approximately 1020°C (Reinaldo, 2004) results in Re_D of 2600. The maximum y^+ found in the calculations is indicated in table 1.

The theoretic Strouhal number, for this Reynolds number, is approximately 0.2 providing an estimative of vortex shedding frequency as 53Hz (0.02 [s]). Based on this, the time step selected was 0.0002 [s] for all cases. Around 20 iterations are required for convergence of the equations, within each time step to within a prescribed tolerance of 10^{-3} for the normalized residuals. Statistics are then collected after 200 time steps, necessary to create the instabilities and some few vortexes shedding, and then all dates presented here were collected with approximately nine shedding cycles.

The boundary conditions used on the exit surface is the convective boundary condition equal to zero. This boundary condition ensures that vortices can approach and pass the flow boundary without significant disturbances or reflections into the inner domain (Breuer, 1998).

Non slip condition is used at solid walls. In the spanwise as in the cross stream direction periodic boundary conditions are assumed. At the inlet flow a plane constant velocity profile is imposed (no perturbations added). We do have in mind that this is not the real conditions of the flow near the heat exchange tubes, but as the LES approach is very suitable to the flow field, the insertion of turbulence intensity can change the conditions from one case to the other making difficult the comparison with calculated or experimental results from other authors.

All the equations are solved using a commercial code FLUENT 6.2.16 that uses a cell centred finite volume method with central differences to solve the incompressible Navier Stokes equations. For the momentum equations the bounded central differencing scheme is used in order to lead to low oscillations in the solution fields, the pressure values at the faces are interpolated using the momentum equation coefficients. The solver is segregated with implicit formulation and the temporal discretization is second order. The pressure velocity coupling is achieved by the use of the SIMPLE algorithm.

4. Results and Discussion

4.1. Gas flow Analysis

In order to show the three dimensionality of the turbulence in bluff body flow for LES simulation the cases A0D, A0S, A1S and A1D are compared with the A2D and A2S. All simulations were done using the same inlet conditions. Fig. 2 shows the time average streamwise velocity along the centreline. Experimental results presented are for a comparable case with $Re_D=3900$.

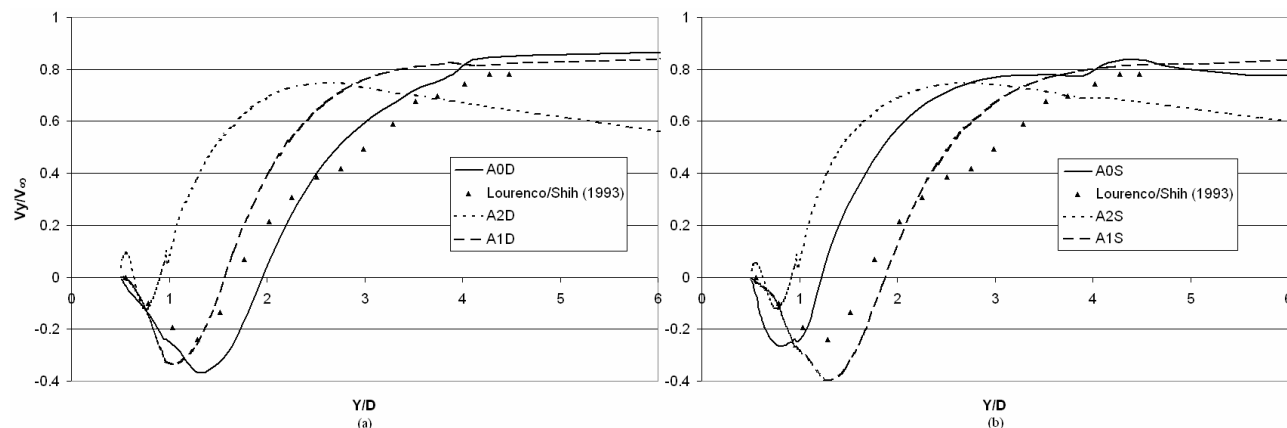


Figure 2. Mean streamwise velocity along the centerline, (a) Dynamic subgrid model; (b) Smagorinsky subgrid model.

As can be seen the run A2D and A2S show a secondary recirculation within the main recirculation in the wake. The extension of the recirculation is under predicted by the grid (A2) with small number of nodes in the spanwise direction as noted by other authors (Breuer, 1998).

The experimental observations were taken from Lourenco and Shih, (1993), *apud* Breuer (1998) and were obtained for a slightly higher Reynolds number (3900) for which the size of the recirculation zone is expected to be smaller. Calculations for a similar Reynolds number, 2580, is presented by Liang and Papadakis (2006) leading to a recirculation zone length, L_r/D of 1.75, close to the A0D and A1S runs.

Once the grid has an insufficient resolution the large eddies became more dependable of the viscosity model and this results in an early transition on the shear layers separating from the cylinder which led to a shorter recirculation zone, the same happened to the run A0S, specially because it used a fixed constant in the model. This grid resolution possibly led to an under prediction of the turbulence in the A1D run resulting in an early separation of the shear layer.

Figure 3 presents a comparison of the streamwise velocity profile across the wake at a distance $Y/D = 1$. The axes are normalized by the free stream velocity and the results in the border of the computational domain the ratio V_y/V_∞ is 1.10 due to the blockage ratio of 16%.

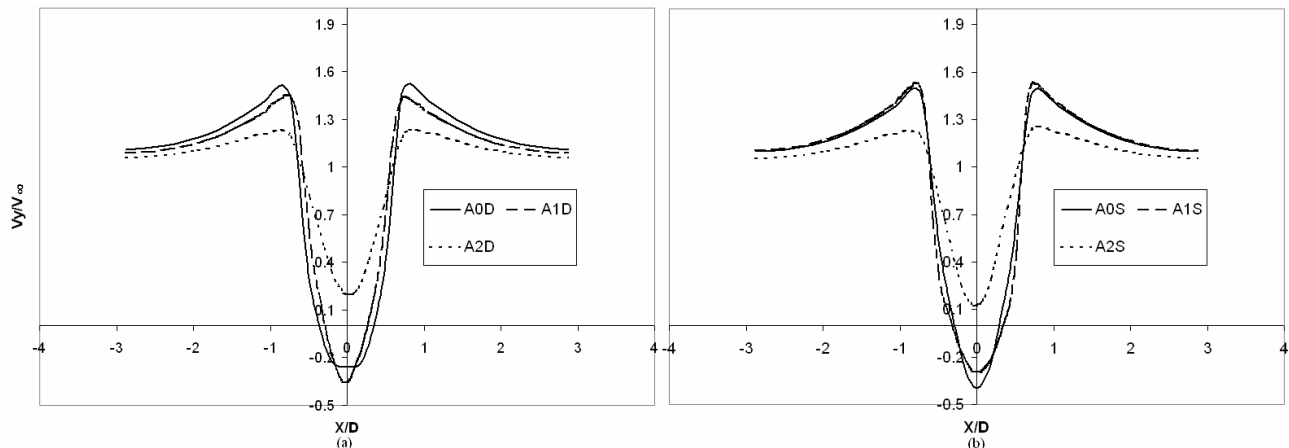


Figure 3. Streamwise velocity in the wake ($Re = 2600$), (a) Dynamic subgrid model, (b) Smagorinsky subgrid model.

Considering the results presented here, the runs used to determine the particle deposition on the tube will be A0D and A1S.

4.2. Particle Flow Analysis

Figure 4 displays the relative rate of $1 \mu m$ particle deposition on the tube for the runs A1S and A0D. The Stokes number for this particle size is $St_p = 1.83 \times 10^{-4}$ which is much smaller than the ratio between the time step in the calculations and the characteristic flow time (10^{-2}) so these particles are influenced by the subgrid turbulence as can be observed from the differences between figures 4a and 4b. The particle deposition rate displayed in Fig. 4 is the number of particle deposited on the wall for sectors of 5° arcs around the tube perimeter. Results concerning the particle phase are averaged over the 625 time steps, which correspond to, roughly, eight shedding vortex thus giving the mean values over this time period.

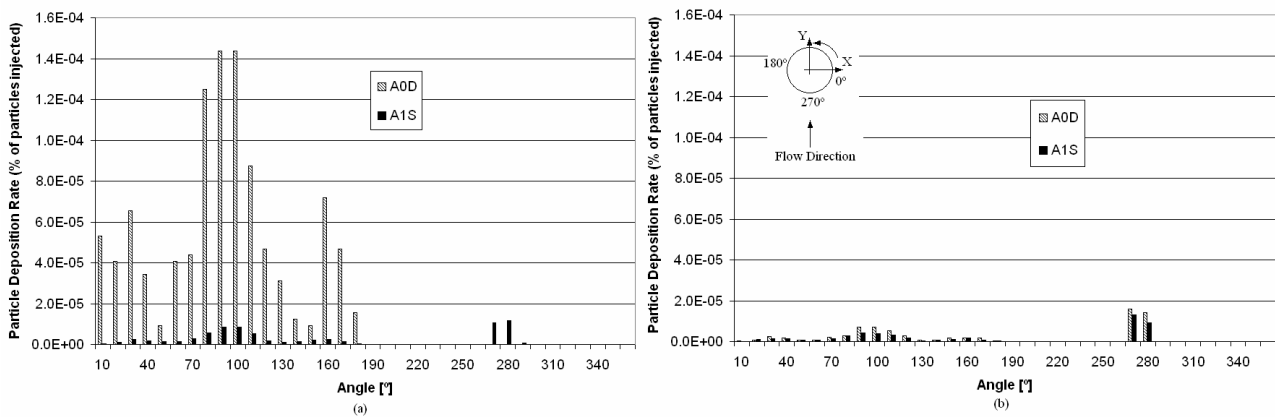


Figure 4. Percentage of particle deposited during the 625 time step for a $1 \mu m$ diameter. (a) with the DRW model, (b) without the DRW model.

As the $1 \mu m$ particle has a very low Stokes number it follows the fluid without slip and most particles congregate in the core regions of the large scale vortex structures. Despite the two grids considered provide similar size of the wake recirculation, the coarser grid, with more turbulent energy simulated in the small scales, leads to a large influence of the DRW model as can be observed. The main impact of the DRW is on the downstream side of the tube, as expected, providing a more coherent rise on the number of particles deposited on the tube. For the heat exchange tube case we are going to consider the run A1S.

4.2. Heat Exchanger Tube

The heat exchanger tube is considered with a uniform surface temperature of 800 K that is the vapour temperature on the outlet of the superheater for the design conditions. All the other boundary conditions are considered as being the same. Fig. 5 shows the impact of considering the heat transfer of the wall on the particle deposition.

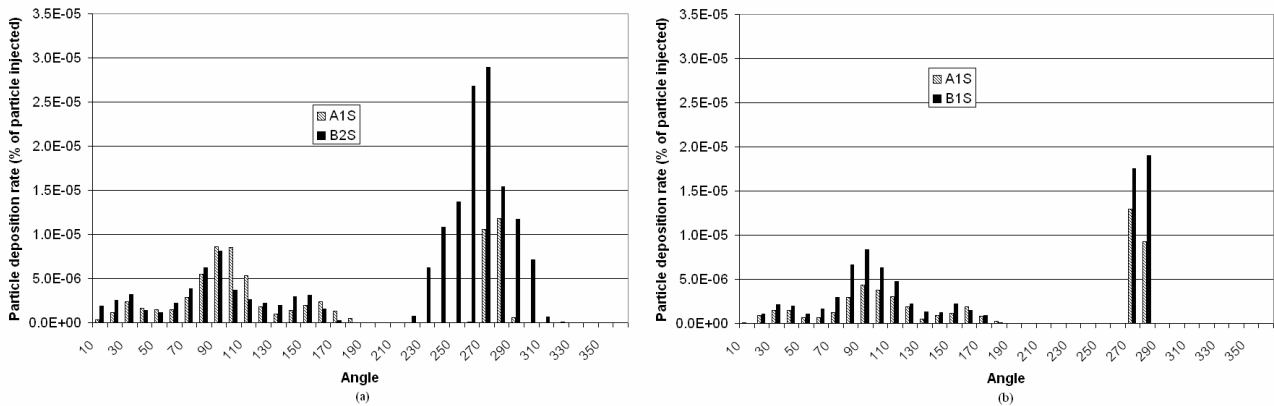


Figure 5. Comparative analysis of the impact on the heated tube on the deposition of the 1µm particle. (a) with DRW, (b) without DRW.

From Fig. 5 it is possible to observe that the heated wall tends to spread the particle deposition in both cases analysed here (with and without the DRW model). Due to the gas cooling the deflection of the flow is lower and hence more particles reach the upstream side of the tube. This leads also to an increase of deposition of this small scale particle, in the upstream side of the tube, while in the wake region the results are not strongly affected.

Fig. 6 presents the distribution of particles hitting the tube for particle sizes 30; 45; 60 and 90 µm. From this figure it is clear that the particle collection efficiency increases with diameter, as expected. The decrease of particle hitting around the tube is consistent with the flow field around it, so the number of particle deposited must be higher on the stagnation point and decreases as the stream lines change around the tube. Nevertheless, on Fig. 6 (a) it is possible to observe that the larger particles have higher impact rates not in the centre of the tube but around $\pm 10^\circ$ from this location. These are the limits of the moving of the stagnation point as the vortex shed from the cylinder. The results show that no large size particles hit the downstream side of the tube. This can be explained by the relatively smaller velocities in the vortices and because the particles are deflected around the tube and can not be captured by the vortices. The minimum Stokes number for 30 µm particles is 0.16 and therefore the particle characteristic time is comparable with the time step in the simulations.

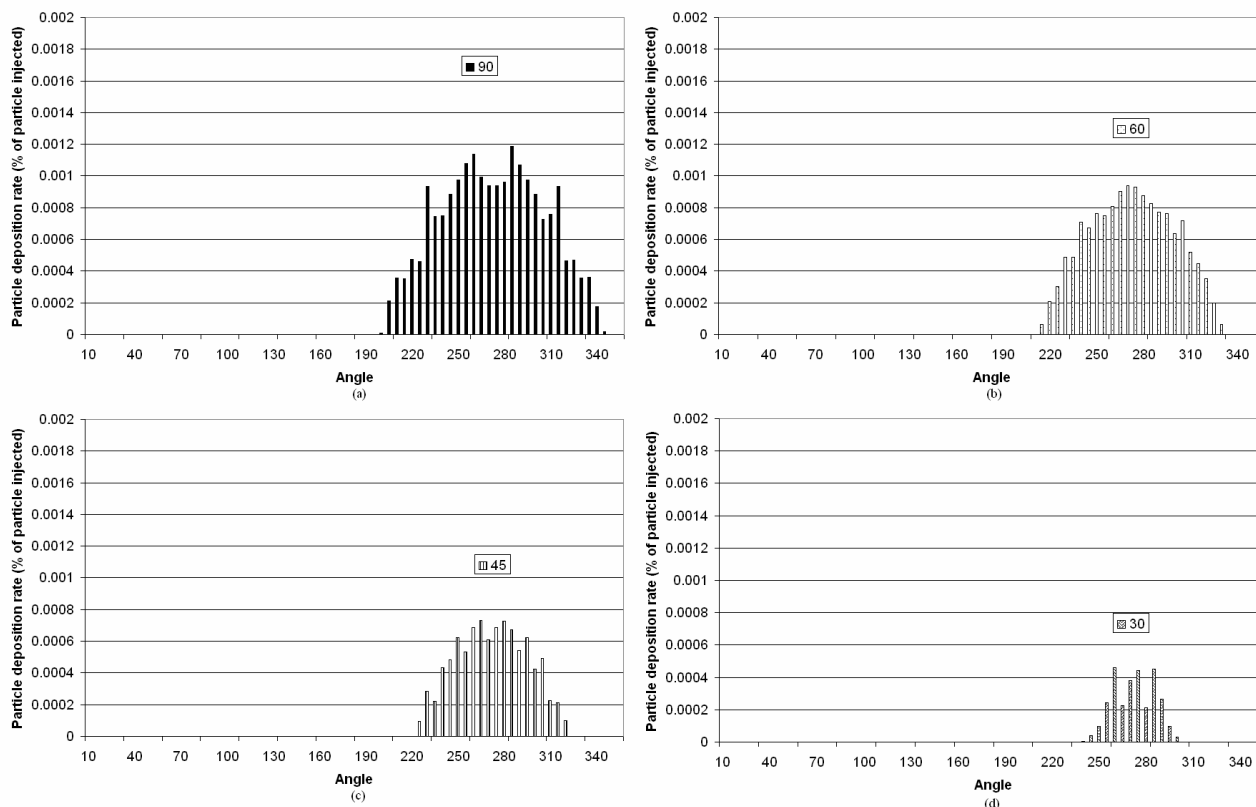


Figure 6. Percentage of particle deposited during the 625 time step. (a) 90 μm diameter, (b) 60 μm diameter, (c) 45 μm diameter, (d) 30 μm diameter.

5. Conclusions

The use of large eddy simulation to solve the flow around a tube is analysed and shown to represent the average flow characteristics. The calculated size of the wake recirculation is sensitive to the spanwise size of the grid. Appropriate selection of the minimum size of the domain and the size of grid close to the walls leads to satisfactory results. The use of 2D domains leads to erroneous results.

The LES calculations provide a basis for the prediction of particle deposition on a heat exchanger tube located inside the boiler. The consideration of gas cooling leads to more disperse distribution of small particles hitting the tube. For the larger particle sizes the expected influence of particle diameter is observed. The results suggest that the particles hitting the upstream side of the tube have more intensity between two positions that correspond to the oscillation of the position of the stagnation point.

The approach presented here can estimate in a good way the particle deposition on the heat exchange tube, supplying the input data to the models that simulate the surface grow.

6. Acknowledgement

Thanks to the Brazilian agencies CNPq (Conselho Nacional de Desenvolvimento Científico e Tecnológico), CAPES (Coordenação de Aperfeiçoamento de Pessoal de Nível Superior) and GRICES (Gabinete de Relações Internacionais da Ciência e do Ensino Superior) for the financial support. Acknowledgement is also given to FCT through project POCTI/EME/47900/2002. Also, special thanks are given to Tractebel Energy and to the Mechanical Engineering Luis Fellipe to permit the easy access to the data of the velocity and temperature as the access to the ash deposit.

7. References

- ANEEL, 2006, (Brazilian Electricity Regulatory Agency), available at www.aneel.gov.br, April.
- Arpaci V.S., 1997, "Microscales of turbulence, heat and mass transfer correlation", Gordon and Breach Science Publishers, Amsterdam, Netherlands.
- Bouris D., Papadakis G., Bergeles G., 2001, "Numerical evaluation of alternate tube for particle deposition rate reduction in heat exchanger tube bundles", International Journal of Heat and Fluid Flow, Vol 22, pp 525 – 536.

- Breuer M., 1998, "Numerical and modeling influences on large eddy simulations for the flow past a circular cylinder", *International Journal of Heat and Fluid Flow*, Vol 19, pp 512 – 521.
- Crowe C.T. 1979, "Gas particle flow", in "pulverized coal combustion and gasification. Theory and applications for continuous flow process", Smoot L.D., and Pratt D.T., (ed.), Plenum Press, New York.
- Fluent (version 6), 2005, User's Guide, Fluent Inc.
- Fröhlich J., Rodi W., Kessler Ph., Parpais S., Bertoglio J.P., Laurence D., 1998, "Large eddy simulation of flow around circular cylinders on structured and unstructured grids". In: Hirschek E., (ed) *Numerical Flow Simulation I. Notes on numerical fluid mechanics*, vol 66, Vieweg, pp319 – 338.
- Franke J., Frank W., 2002 "Large eddy simulation of the flow past a circular cylinder at $Re_D=3900$ ", *Journal of Wind Engineering and Industrial Aerodynamics*, Vol 90, pp 1191 – 1206.
- Germano M., Piomelli U., Moin P., Cabot W., 1991 "A dynamic subgrid scale eddy viscosity model", *Phys Fluids A*, Vol 3, pp 1760 – 1765.
- Knudsen, S., K., 2001, "Numerical investigation of ash deposition in straw-fired boilers - Using CFD as the framework for slagging and fouling predictions", PhD Thesis, Institute of Energy Technology, Aalborg University, Denmark.
- Liang C., Papadakis G., 2006, "Large eddy simulation of pulsating flow over a circular cylinder at a subcritical Reynolds number", *Computers and fluids*, vol 35, Article in press.
- Lübcke H., Schmidt St., Rung T., Thiele F., 2001, "Comparison of LES and RANS in bluff body flow", *Journal of Wind Engineering and Industrial Aerodynamics*, Vol 89, pp 1471 – 1485.
- Mendes, L.J.N., Forgerini, F. L., Figueiredo, W., Bazzo, E., Azevedo, J.L.T., 2006, "Comparison analysis of boiler ash deposit and porous structure simulated by the ballistic model", *ECOS 2006*, Crete Greece, July, pp 12-14.
- Reinaldo R. F., 2004 "Estudo numérico de transferência de calor e deposição de cinzas em caldeiras de carvão pulverizado", Doctoral thesis, Federal University of Santa Catarina, Florianópolis, Brasil, 2004.
- Saugaut P., Grohens R., 1999, "Discrete filters for large eddy simulation", *International Journal for Numerical Methods in Fluids*, vol 31, pp 1195 – 1220.
- Silveira N.A., 2002, "Simulação de grandes escalas de escoamentos turbulento" in *Turbulência: Anais da I escola de primavera em transição e turbulência*, Silva A.P.F., Menut P.P.P., Su J., (ed.), ABCM publisher, Rio de Janeiro, in Portuguese.